NeuroImage 323 (2025) 121611

Contents lists available at ScienceDirect

NeuroImage

journal homepage: www.elsevier.com/locate/ynimg

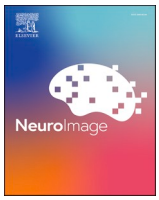

Cerebral perfusion during pharmacologically induced sleep: Cortical and subcortical changes quantified by ASL MRI

Balázs Örzsik [a,b,*], Iris Asllani [b,c], Derk-Jan Dijk [d,e], Neil A Harrison [f], Mara Cercignani [f,b]

[a] Radiology, Leiden University Medical Center, Leiden, Netherlands
[b] CISC, Brighton and Sussex Medical School, Brighton, United Kingdom
[c] Rochester Institute of Technology, NY, United States
[d] Surrey Sleep Research Centre, Faculty of Health and Medical Sciences, University of Surrey, Guildford United Kingdom
[e] UK Dementia Research Institute Care Research and Technology Centre, Imperial College London and the University of Surrey, Guildford UK
[f] CUBRIC, Cardiff University, United Kingdom

ARTICLE INFO

Keywords:
Sleep neuroimaging
Cerebral blood flow
ASL
Neurometabolism

ABSTRACT

Introduction: Cerebral blood flow (CBF) reductions during non-REM sleep have been consistently demonstrated in positron emission tomography (PET) studies, but PET's limitations restrict its use. Arterial spin labeling (ASL) MRI allows repeated, noninvasive CBF measurement but has rarely been applied to sleep. This study examined global and regional CBF changes during wakefulness and pharmacologically induced sleep after sleep deprivation, with an exploratory focus on the ascending arousal network (AAN).

Methods: Twenty-one healthy participants (13 male, 8 female; mean age = 22.4 ± 3.1 years) underwent ASL MRI during wake and sleep. Sleep was facilitated with 10 mg Zolpidem following sleep deprivation and verified through reduced button-press responses and increased high-frequency heart rate variability (HF-HRV). Pseudo-continuous ASL was acquired with a labeling duration of 1.9 s and post-labeling delay of 1.8 s.

Results: Sleep was confirmed in 19 participants; one was excluded for excessive head displacement, resulting in a final sample of 18. Grey matter CBF decreased from 59.7 ± 9.0 to 49.5 ± 8.1 ml/100*g*/min ($p < 0.0001$), and white matter CBF from 28.7 ± 4.9 to 25.1 ± 3.0 ml/100*g*/min ($p < 0.001$). Voxelwise analysis revealed reductions in cingulate, medial prefrontal cortex, precuneus, insula, thalamus, and caudate. ROI analysis indicated decreases in AAN regions including the Locus Coeruleus (−29.3 %, $p = 0.0019$), Medial Reticular Formation (−22.8 %, $p = 0.0010$), Pontis Oralis (−23.4 %, $p = 0.0044$), and Pedunculopontine Nucleus (−20.8 %, $p = 0.0023$).

Discussion and Conclusion: Observed perfusion decreases are consistent with PET evidence of cortical and thalamic downregulation during sleep and indicate suppression of brainstem arousal nuclei. These findings provide a detailed ASL characterization of cortical and brainstem perfusion changes during pharmacologically induced sleep, extending PET work and offering new insight into sleep-related arousal systems.

1. Introduction

Sleep is a fundamental biological process that is highly conserved across both mammalian and non-mammalian species (Zimmerman et al., 2008). Despite its universality, the primary functions and underlying mechanisms of sleep remain unresolved. Understanding why sleep is necessary and what critical functions occur during sleep that cannot happen during wakefulness is crucial. Even modest periods of sleep deprivation can impair cognitive and physical performance and disrupt emotional regulation (Alhola and Polo-Kantola, 2007; Wickens et al., 2015; Palmer and Alfano, 2017). Chronic sleep loss has also been associated with increased levels of stress hormones, elevated blood pressure, compromised immune function, and heightened vulnerability to various psychiatric and somatic disorders (Luyster et al., 2012).

Over the years, several hypotheses have emerged to explain the functions of sleep, including synaptic downscaling, memory consolidation, metabolic regulation, and energy conservation (Tononi and Cirelli, 2014; Buzsáki, 1998; Rechtschaffen and Bergmann, 2002; Stephenson, Chu and Lee, 2007). The latter hypothesis has long been supported by data showing that non-REM sleep, particularly slow-wave sleep (SWS),

* Corresponding author at: Radiology, Leiden University Medical Center, Albinusdreef 2, 2333 ZA, Leiden, Netherlands.
E-mail address: b.orzsik@lumc.nl (B. Örzsik).

https://doi.org/10.1016/j.neuroimage.2025.121611
Received 28 September 2025; Received in revised form 19 November 2025; Accepted 22 November 2025
Available online 23 November 2025

is associated with decreased cerebral glucose metabolism and reduced neuronal activity (Buchsbaum et al., 2001; Nofzinger et al., 2002). More recently, the brain clearance hypothesis has gained significant attention. This theory proposes that sleep facilitates the removal of metabolic waste from the brain via the glymphatic system, a clearance mechanism that is closely tied to cerebrovascular and interstitial fluid dynamics (Iliff and Nedergaard, 2013; Fultz et al., 2019; Xie et al., 2013).

Studies investigating cerebral blood flow (CBF) during sleep have provided crucial support for the metabolic regulation and energy conservation theory of sleep. Positron emission tomography (PET) studies have consistently reported widespread reductions in CBF during SWS, particularly in regions like the thalamus, frontal cortex, and basal ganglia that are involved in wakefulness and slow wave activity (SWA) generation (Braun et al., 1997; Maquet et al., 1997; Andersson et al., 1998; Kajimura et al., 1999). Complementing these findings, Elvsåshagen et al. (2019) used arterial spin labeling (ASL) MRI to demonstrate that CBF decreases from pre- to post-sleep in regions implicated in attentional and executive functions, suggesting a restorative downscaling in functional demands following sleep. During SWS, CBF reductions are thought to reflect lower metabolic demands during the extended hyperpolarizing "off" periods between neuronal bursts. Moreover, EEG-PET studies have shown negative correlations between SWA and CBF, particularly in frontal and thalamic regions (Hofle et al., 1997; Dang-Vu et al., 2005), reinforcing the role of these areas in the generation and modulation of deep sleep.

With the exception of a single study by Tüshaus et al. (2017) which measured CBF during sleep using ASL in combination with EEG, most prior work on sleep-related perfusion changes has relied on PET imaging. While PET is often considered the gold standard for quantifying absolute CBF, its use is limited by high cost, the need for a nearby cyclotron, specialized staff for injections, and logistical challenges that complicate repeated or prolonged sleep recordings. In contrast, ASL is a non-invasive MRI technique that does not require contrast agents or radiation and is better suited for extended scanning sessions in naturalistic sleep settings. Although Elvsåshagen et al. (2019) also used ASL, participants in that study did not sleep in the scanner; rather, CBF was measured before and after sleep, limiting insight into the dynamic changes occuring during sleep itself. Thus, the study by Tüshaus et al. remains the only published work to date directly capturing sleep-state-dependent CBF with ASL.

Here, we sought to extend the existing literature by using ASL to investigate CBF changes during human sleep induced via a combination of sleep deprivation and pharmacological intervention (Zolpidem, 10 mg). This approach ensured high sleep pressure and increased likelihood of achieving consolidated non-REM sleep in the scanner. We hypothesized that sleep would be associated with both global and region-specific reductions in CBF, particularly in areas known to be involved in slow-wave generation, such as the thalamus, basal ganglia, and brainstem.

This study is also part of a broader multimodal MRI investigation into the effects of sleep on glymphatic function. Previous results from this dataset, including diffusion kurtosis findings indicative of tissue microstructural changes during sleep, were published in Örzsik et al., 2023. Here, we present ASL-based perfusion findings, including a focused exploratory analysis of the ascending arousal network (AAN), a brainstem system critical for regulating wakefulness and transitions between sleep and arousal states (Edlow et al., 2012). Given the AAN's influence on neuromodulatory tone, particularly through noradrenergic signaling, and the proposed role of noradrenaline as a master regulator of the glymphatic system, these findings offer novel insights into how reduced activity in arousal-related brainstem pathways may contribute to sleep-dependent brain clearance.

2. Methods

2.1. Ethics statement

Ethical approval for this study was obtained from the Brighton and Sussex Medical School Research and Governance Ethics Committee (ER/BO80/1), and all procedures were conducted in accordance with the Declaration of Helsinki. All participants provided written informed consent prior to enrolment and received financial compensation for their participation.

2.2. Participants

Participants are the same as reported in Örzsik et al., 2023, and consisted of 21 healthy adults (15 males and 6 females; mean age = 22.3 ± 3.2 years) recruited through university-wide advertisements. All participants underwent a comprehensive screening process, including a detailed medical questionnaire focusing on contraindications to Zolpidem, as well as assessments for any history of somatic or psychiatric illness, substance abuse, or known sleep disorders. Standard MRI exclusion criteria also applied. To assess baseline sleep quality, participants completed the Pittsburgh Sleep Quality Index (PSQI) (Buysse et al., 1989).

2.3. Study design

We employed a within-subject, crossover design in which all participants completed two MRI sessions, one in the awake state and one during sleep deprivation followed by pharmacologically induced sleep, scheduled 3 to 7 days apart (mean = 4.0 days); summarized in Fig. 1. Although the session order was intended to be randomized, practical constraints such as participant availability and preference were taken into account when scheduling. As a result, fourteen participants (67 %) completed the awake session first.

To minimize the influence of circadian rhythms, both sessions were scheduled at approximately the same time of day (mean start time = 09:44 ± 22 min). For the wake session, participants were instructed to arrive well-rested after a full night's sleep. For the sleep session, they underwent ~24 h of sleep deprivation and were administered 10 mg of Zolpidem 30 min prior to scanning. Zolpidem is a short-acting non-benzodiazepine hypnotic known for its efficacy in inducing and maintaining sleep, with peak plasma concentrations reached within 45 min and a half-life of 1.5–2.4 h (Priest et al., 1997; Monti et al., 2017). Participants were instructed to avoid caffeine and nicotine for 12 h before each scan.

Fig. 1 provides an overview of the study design and timing of assessments. Sleep-wake patterns were monitored using actigraphy (Actiwatch Spectrum Plus, Philips Respironics) for 24 h preceding each scan. Subjective sleepiness was assessed immediately before scanning using the Karolinska Sleepiness Scale (KSS) (Åkerstedt and Gillberg, 1990). During scanning, participants were asked to maintain light pressure on a button box to detect reductions in muscle tone as a behavioural proxy for sleep onset. In addition, physiological signals—including respiration (via a Biopac respiration belt) and cardiac pulse (via a Nonin 8600FO pulse oximeter) were continuously monitored and recorded using Biopac AcqKnowledge 5 software. Following each scan, participants completed Likert scale–based subjective sleep questionnaire rating how long, how deeply, and at what point during the scan they believed they had fallen asleep.

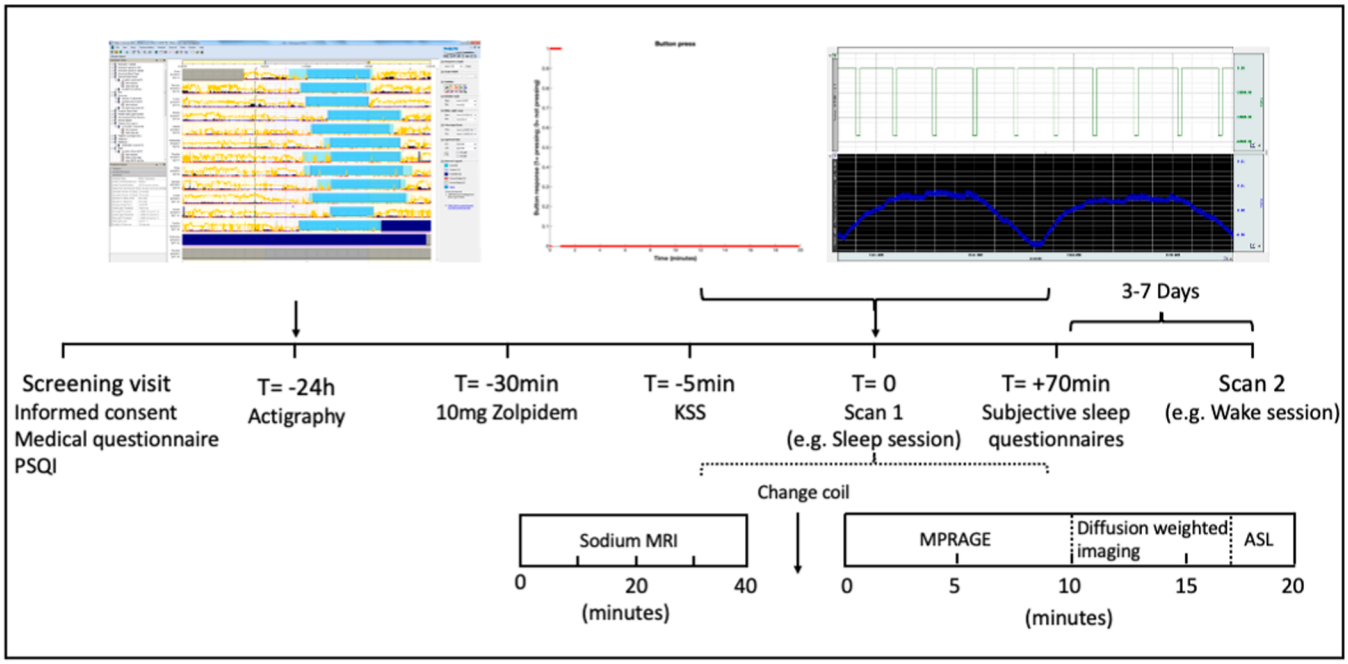

Fig. 1. Overview of study design. Example shown depicts a participant whose protocol began with the sleep session. (Modified from Örzsik B., 2022.).

2.4. MRI acquisition

All MRI data were acquired on a 3T Siemens Prisma scanner (Siemens Healthineers, Erlangen, Germany) equipped with a 32-channel phased-array head coil. Cushioning pads were used to minimize head motion during scanning. Each session included sodium imaging (a non-invasive MRI technique that images sodium ions naturally present in tissue, requiring no injections or contrast agents; these data were the object of a different research question, not reported in this study), T1-weighted anatomical imaging (volume-based morphometry, results reported in Örzsik et al., 2023), diffusion MRI (reported in Örzsik et al., 2023), and pseudo-continuous arterial spin labeling (pCASL).

The T1-weighted anatomical scan was obtained using an MPRAGE sequence with the following parameters: TR = 2.3 s, TE = 2.19 ms, TI = 920 ms, flip angle = 9°, matrix = 256 × 256 × 192, and isotropic voxel size of 1 mm^3.

For CBF measurement, pCASL was employed using background suppression and the following acquisition parameters: labeling duration = 1900 ms, post-labeling delay (PLD) = 1800 ms, TR = 5 s, TE = 14 ms, in-plane resolution = 3.5 × 3.5 mm^2, slice thickness = 6 mm, and 18 axial slices. Each ASL scan included 20 label-control pairs, and a separate M0 image was acquired for each participant using the same readout parameters for absolute quantification of perfusion. Perfusion-weighted images were processed according to consensus recommendations (Alsop et al., 2015) for quantifying CBF from ASL data.

2.5. Image processing

SPM12 (www.fil.ion.ucl.ac.uk/spm/software/spm12) and in-house developed Matlab scripts were used for image processing and statistics. Rigid-body motion correction was used to realign labelled and control images (20 pairs per session). Framewise displacement (FD) was calculated, and the mean FD values across the two conditions (wake and sleep) were compared using a paired *t*-test. Perfusion weighted images were calculated for each control-labelled pair by subtracting the labelled image from the control. The mean perfusion-weighted images (wake and sleep) were converted to absolute CBF using the standard one-compartment model and parameter assumptions recommended in the ASL consensus paper (Alsop et al., 2015), and registered to the same high resolution T1-weighted anatomical image. The spatial normalization parameters derived from the segmentation of the T1 image, which transform it into MNI space at 2 mm isotropic resolution, were then applied to the CBF maps using 7th degree b-spline interpolation.

2.6. Brain-wide CBF analysis

Individual grey matter (GM) and white matter (WM) tissue probability maps (TPMs) were obtained by segmentation of the T1-weighted anatomical image (MPRAGE) in SPM12. The normalization parameters from this segmentation, were applied to the TPMs using 7th degree b-spline interpolation. For each tissue class, a group mean TPM was calculated across participants, thresholded at > 0.7, and binarized to create GM and WM binary masks. These masks were applied to the normalized CBF images to extract mean GM and whole-brain CBF values for each participant. A one-tailed paired *t*-test in MATLAB was used to compare global averages between wake and sleep sessions, with $p < 0.05$ considered statistically significant.

2.7. Whole brain voxel-wise CBF analysis

The normalized (MNI) and smoothed (FWHM=4 mm) CBF images were compared between sessions (wake vs sleep) using a voxel wise paired-sample *t*-test (SPM12). The statistical significance was determined using cluster size inference with an initial cluster forming threshold of $p < 0.001$, where clusters with Family-wise Error (FWE)-corrected $p < 0.05$ were considered significant. Percentage change was determined for each participant before averaging in the following way: ((mean cluster sleep CBF - mean cluster wake CBF)/mean cluster wake CBF) *100; ± represents SD between participants. Anatomical information was derived using the xjView toolbox (http://www.alivelearn.net/xjview), in Table 1 "aal3" denotes Automated Anatomical Labeling (Rolls et al., 2019).

2.8. Exploratory ROI analysis in ascending arousal network

Paired *t*-test analysis was carried out to compare mean CBF signal in Harvard Ascending Arousal Network (AAN) Atlas ROIs (Edlow et al., 2012). The AAN atlas includes the following nuclei: Dorsal Raphé (296

mm^3 corresponding to ~4 ASL voxels), Locus Coeruleus (112 mm^3; ~2 ASL voxels), Median Raphé (184 mm^3; ~3 ASL voxels), Medial Reticular Formation (376 mm^3; ~5 ASL voxels), Periaqueductal grey (488 mm^3; ~7 ASL voxels), Parabrachial complex (138 mm^3; ~2 ASL voxels), Pontis Oralis (256 mm^3; ~4 ASL voxels), Pendunculopontine nucleus (144 mm^3; ~2 ASL voxels) and Ventral Tegmental Area (64 mm^3; ~1 ASL voxel). Significance was determined at alpha= 0.05 after Bonferroni correction.

2.9. Analysis of physiological measures

Heart rate (HR) and heart rate variability (HRV) were derived from pulse oximeter RR intervals. These data were imported into Kubios software (Kubios Oy, Finland) to extract high-frequency (HF-HRV) components, indicative of parasympathetic activity, in contiguous 5-minute epochs. Changes in high-frequency heart rate variability (HRV-HF) and button press responses were examined using repeated-measures ANOVA in SPSS 27 (IBM Corp.). Main effects of time and condition (wake vs. sleep), as well as their interaction, were assessed.

3. Results

3.1. Participant inclusion

Of the 21 participants recruited, three were excluded from the final analysis: one due to substantial displacement within the head coil during the sleep scan and two for failing to fall asleep. Thus, the final dataset included 18 participants (13 males, mean age = 22.4 ± 3.1 years). The final sample had a mean PSQI score of 4.0 ± 2.3, indicative of generally good sleep quality. The two "non-sleepers" were analyzed separately to explore the effect of the sleep-inducing protocol in the absence of sleep.

3.2. Sleep induction and compliance

Actigraphy measures demonstrated that participants complied with sleep deprivation, 15 out of 18 participants did not sleep at all before the sleep scan, however 3 participants slept on average 4 h 13 min ± 45 min, yet they were able to sleep during the scan. Before the wake scan, participants slept on average 6.59 ± 1.24 h, which was significantly more than their sleep before the sleep scan (0.71 ± 1.45 h), Wilcoxon signed-rank test: $Z = 3.72$, $p < 0.0001$. Evidence for the effectiveness of sleep deprivation was also reflected in the Karolinska Sleepiness Scale (KSS) scores: participants were significantly sleepier before the sleep scan (mean KSS = 7.7 ± 1.0) than before the wake scan (mean KSS = 3.6 ± 1.4), $t(17) = 10.42$, $p < 0.0001$.

3.3. Evidence of sleep during scanning

Behavioural and physiological measures confirmed that participants successfully entered sleep during the sleep scan session, as previously reported in Örzsik et al., 2023. Participants exhibited a marked reduction in button press responses during the sleep scan compared to the wake scan, reflected in a significant Time × Condition interaction ($F(3, 45) = 9.537$, $p < 0.001$; Fig. 2**A**). Additionally, high-frequency heart rate variability (HF-HRV), a marker of parasympathetic activity was significantly elevated during the sleep scan (Time × Condition interaction: $F(1.735, 26.024) = 4.773$, $p = 0.021$, Greenhouse-Geisser corrected; Fig. 2**B**). Heart rate (HR) did not significantly differ between wake (mean ± SD: 63.3 ± 12.4 bpm) and sleep (62.3 ± 13.7 bpm; $t(17) = 0.604$, $p = 0.554$).

3.4. Motion during ASL acquisition

FD did not significantly differ between wakefulness (mean ± SD: 0.22 ± 0.14) and sleep (0.22 ± 0.07; $t(17) = 0.751$, $p = 0.463$). These results suggest that head motion was comparable across the two conditions.

3.5. Brain-wide CBF reductions

Visual inspection of mean CBF maps revealed a widespread reduction in cortical perfusion during sleep compared to wake (Fig. 3). This decrease was observed globally across the brain, with especially pronounced reductions in the anterior and posterior cingulate cortices, orbitofrontal cortex, precuneus, insula, caudate nucleus, hippocampus, and thalamus.

Quantitatively, GM CBF during wakefulness was 59.7 ± 9.0 ml/100 g/min, significantly reduced to 49.5 ± 8.1 ml/100 g/min during sleep (paired *t*-test: $t(17) = 5.545$, $p < 0.0001$), representing a 17.0 % reduction. In WM, CBF decreased from 28.7 ± 4.9 ml/100 g/min during wake to 25.1 ± 3.0 ml/100 g/min during sleep (paired *t*-test: $t(17) = 4.653$, $p < 0.001$), corresponding to a 12.7 % reduction (Fig. 4).

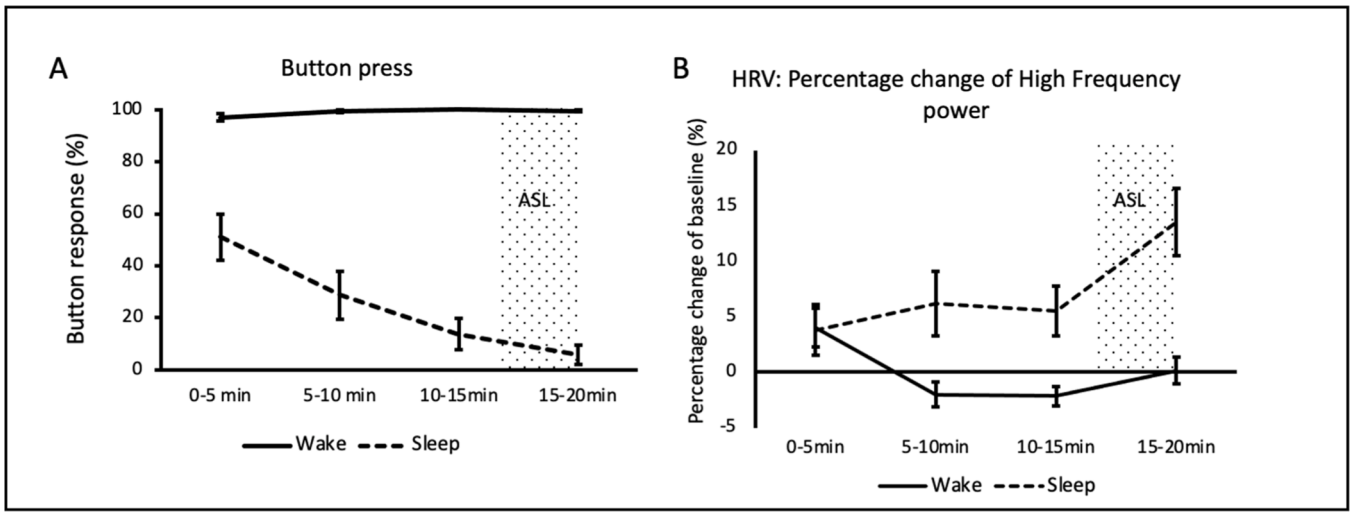

Fig. 2. Behavioural and physiological results. **(A)** Button press during the proton scan sessions (sodium not shown here), the dotted area represents the duration of the ASL scan and the relative position with respect to the start of proton scan; **(B)** High frequency power of HRV during sessions; Error bars = Standard error of the mean. (Figure modified from Örzsik et al., 2023).

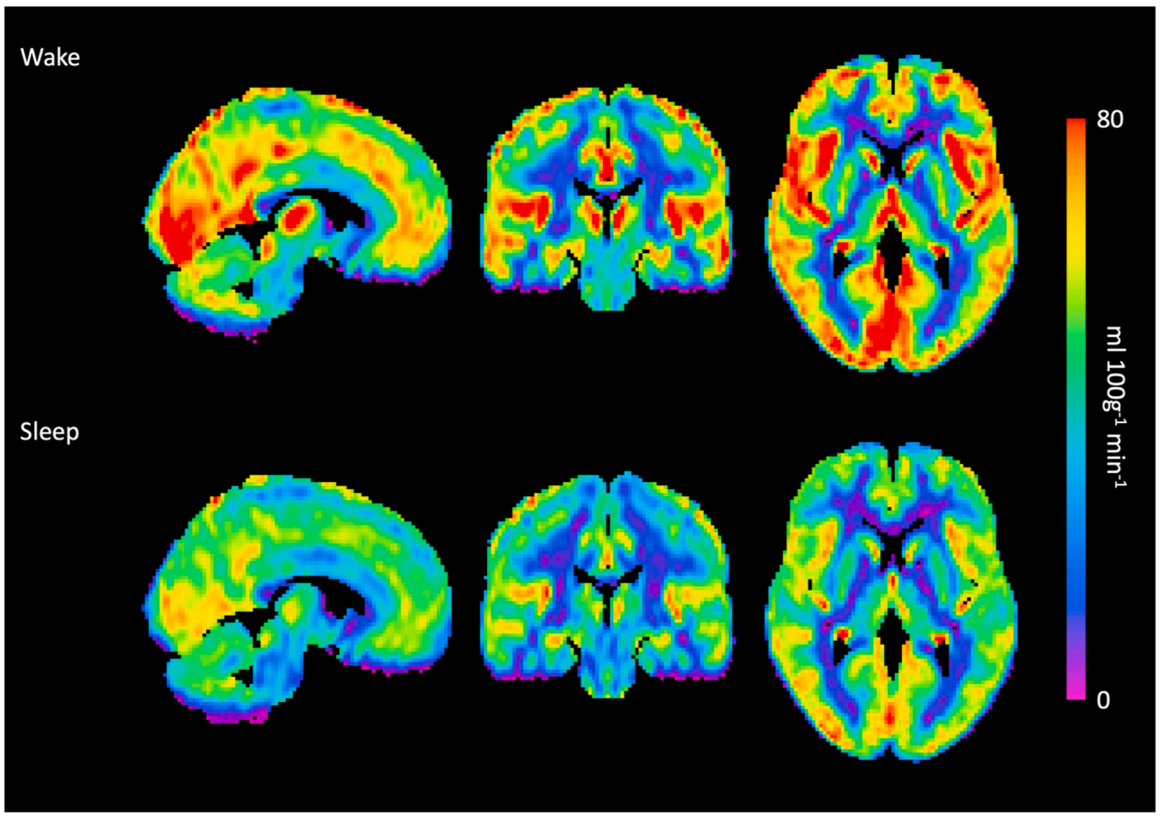

Fig. 3. Illustration of group-level mean cerebral blood flow ($N = 18$) during wake and sleep scans. Displayed slices were positioned at MNI: x = 6 y= −22 $z = 4$.

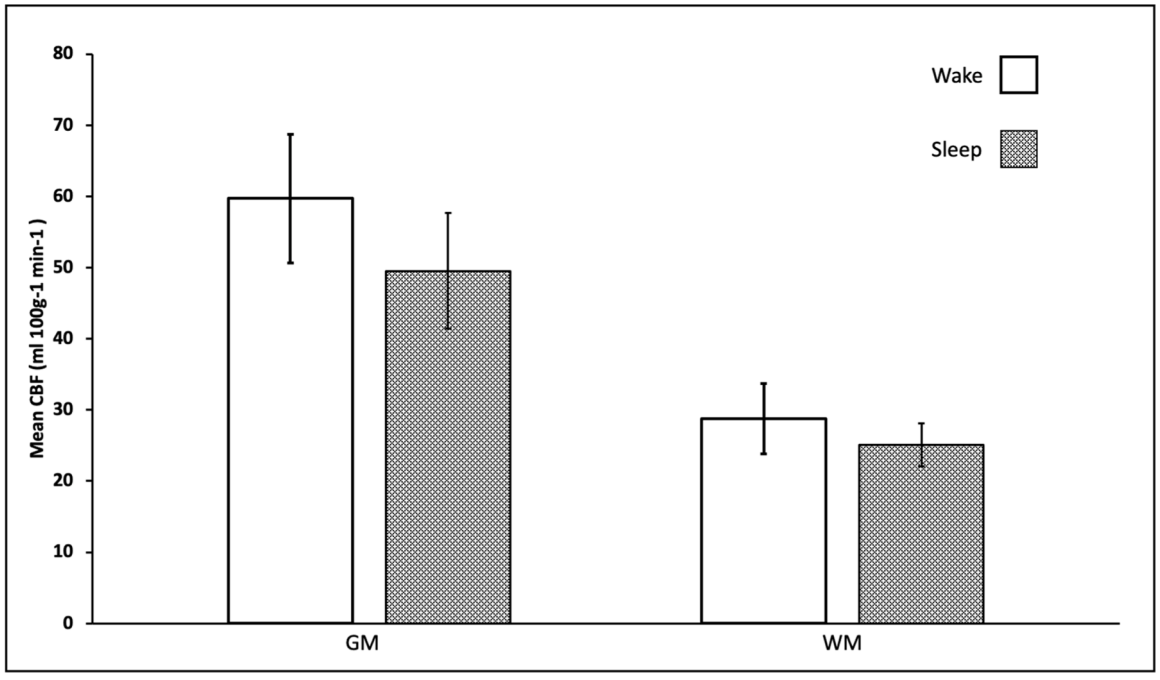

Fig. 4. Representation of global CBF reduction in grey matter (GM; including subcortical regions) and white matter (WM), error bars show standard deviation.

3.6. *Voxelwise analysis of sleep-related CBF changes*

A voxelwise paired *t*-test comparing wake and sleep sessions revealed significant clusters of reduced CBF during sleep across widespread cortical and subcortical regions (Fig. 5). Peak reductions were observed in the anterior and posterior cingulate cortex, orbitofrontal and medial prefrontal cortex, precuneus, insula, thalamus, and caudate nucleus—regions typically active during wakefulness and associated with arousal, attentional control, and integrative processing. A detailed summary of all significant clusters, including anatomical labels, peak MNI coordinates, t-values, and percentage change in CBF, is presented in Table 1.

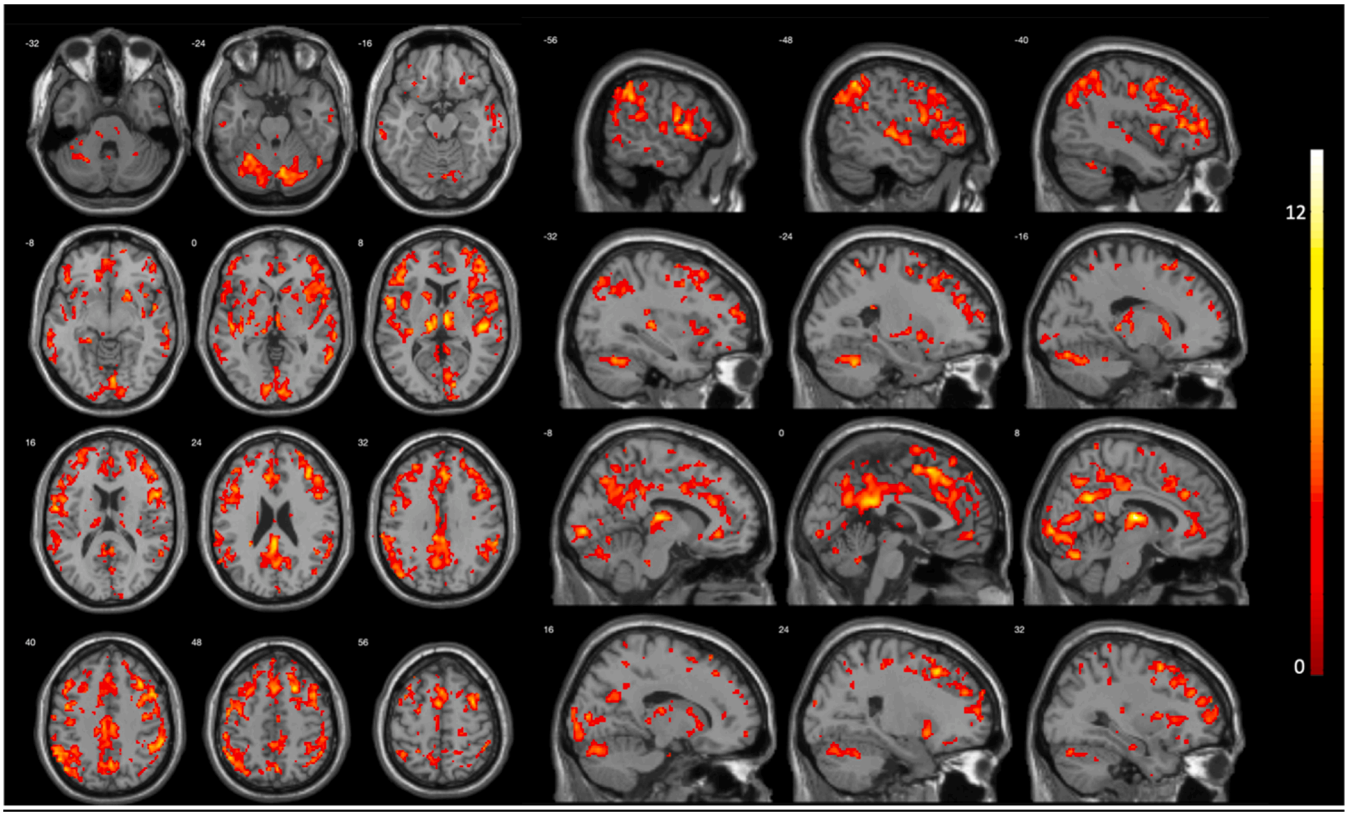

Fig. 5. Voxel-wise comparison of regional CBF between wake and sleep (comparison between the two sessions). Brain regions with significantly reduced CBF during sleep. The statistical significance was determined using cluster size inference with an initial cluster forming threshold of $p < 0.001$, where clusters with a corrected FWE corrected $p < 0.05$ were considered significant. The colour bar represents T-value.

3.7. Exploratory ROI analysis in ascending arousal network

Fig. 6 displays the regional changes in cerebral blood flow (CBF) within key nuclei of the ascending arousal network between wakefulness and sleep. Significant reductions in CBF were observed in the Locus Coeruleus, mean CBF decreased from 39.47 ± 13.93 ml/100 g/min during wakefulness to 27.88 ± 12.27 ml/100 g/min during sleep, corresponding to a 29.33 % reduction ($t(17) = 3.34$, $p = 0.0019$). The Medial Reticular Formation exhibited a reduction from 56.20 ± 16.98 ml/100 g/min to 43.37 ± 9.53 ml/100 g/min, amounting to a 22.81 % decrease ($t(17) = 3.65$, $p = 0.0010$). Similarly, the Pontis Oralis showed a decline in CBF from 43.66 ± 13.44 ml/100 g/min to 33.45 ± 11.80 ml/100 g/min, indicating a 23.41 % reduction ($t(17) = 2.96$, $p = 0.0044$). Finally, the Pedunculopontine Nucleus demonstrated a decrease from 44.75 ± 15.21 ml/100 g/min during wake to 35.44 ± 10.03 ml/100 g/min during sleep, representing a 20.80 % reduction ($t(17) = 3.26$, $p = 0.0023$). These results underscore the broad down-regulation of brainstem arousal centers during sleep.

Table 1
Clusters showing significant reduction in CBF during sleep.

Brain regions	MNI [x y z]	k	T value	p (FWE-corr) cluster	% Change of baseline (mean ± SD)
Thal_MDl_R (aal3v1)	[6 −12 10]	29,116	13.56	<0.0001	−26.3 ± 10.4
Thal_VL_L (aal3v1)	[−12 −18 10]		10.85		
Frontal_Mid_2_R (aal3v1)	[42 10 44]		10.66		
Putamen_R (aal3v1)	[22 12 −8]	296	6.96	<0.0001	−24.0 ± 12.6
Caudate_R (aal3v1)	[12 12 8]		5.41		
Caudate_R (aal3v1)	[14 18 0]		5.04		
Caudate_L (aal3v1)	[−18 14 4]	286	6.86	<0.0001	−25.0 ± 17.4
Putamen_L (aal3v1)	[−12 12 10]		5.94		
Putamen_L (aal3v1)	[−24 4 −4]		5.24		
Temporal_Mid_L (aal3v1)	[−58 −62 −4]	432	6.58	<0.0001	−28.8 ± 20.4
Temporal_Mid_L (aal3v1)	[−66 −30 −6]		5.92		
Temporal_Mid_L (aal3v1)	[−64 −40 −6]		5.89		
Hippocampus	[−20 −36 −6]	51	6.49	0.002	−24.5 ± 12.8
Hippocampus	[−28 −36 −8]		4.96		
Paracentral_Lobule_L (aal3v1)	[−12 −30 62]	61	5.83	<0.0001	−32.9 ± 19.9
Postcentral_L (aal3v1)	[−24 −30 60]		4.39		
Postcentral_L (aal3v1)	[−40 −18 42]	119	5.75	<0.0001	−24.7 ± 18.0
Postcentral_L (aal3v1)	[−34 −22 38]		3.83		
Occipital_Mid_R (aal3v1)	[38 −72 28]	83	5.60	<0.0001	−21.2 ± 12.1
Occipital_Mid_R (aal3v1)	[36 −72 38]		3.56		
Postcentral_R (aal3v1)	[22 −30 54]	75	5.04	<0.0001	−24.9 ± 16.7
Postcentral_R (aal3v1)	[18 −32 63]		3.96		

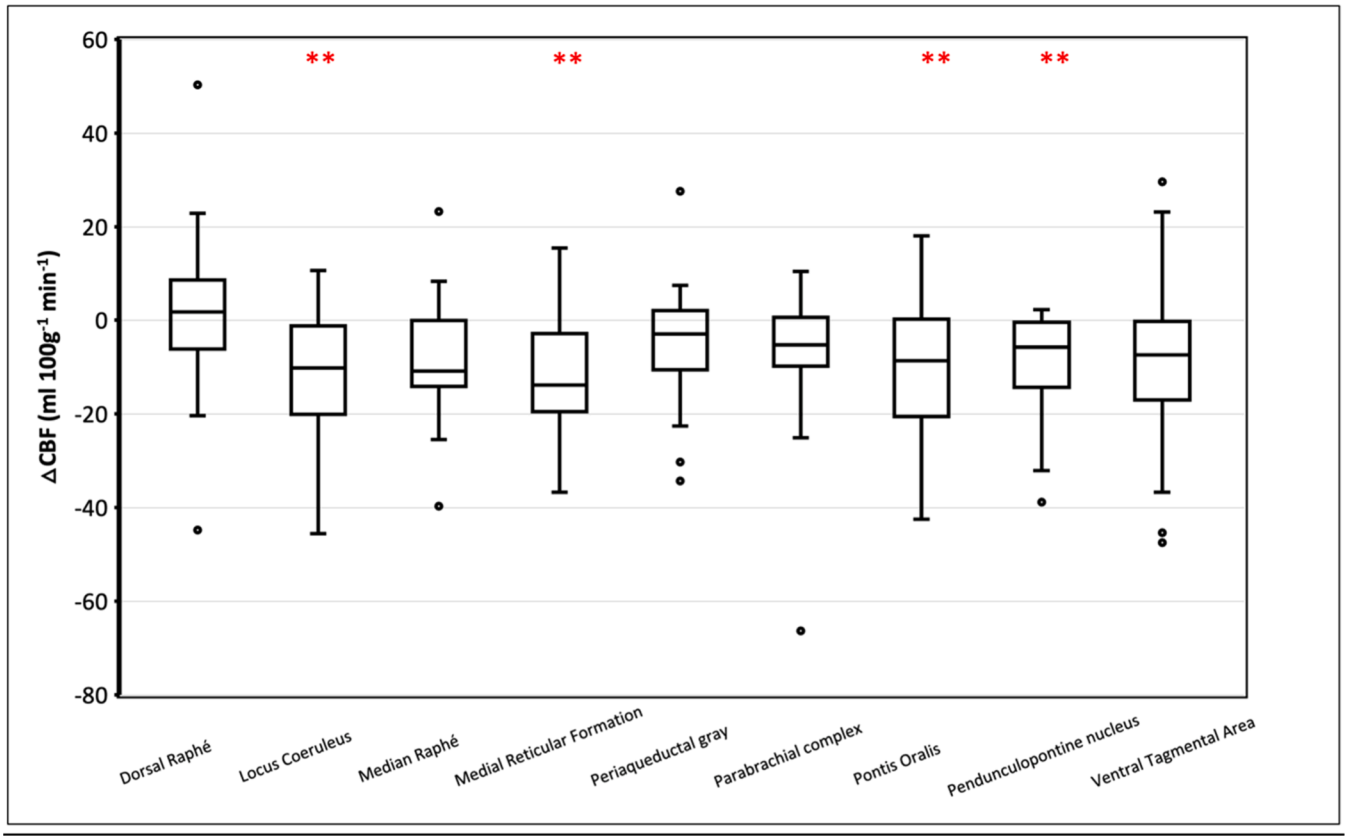

Fig. 6. Box plots CBF change during sleep; line represents the median; box indicates the 25th and 75th percentiles; whiskers show 5th and 95th percentiles; black dots show the outliers; double red stars represent the significant ROIs after Bonferroni correction.

3.8. Non-sleepers — investigation of the effects of the sleep-inducing protocol on CBF and HF-HRV

In the two non-sleepers, global GM CBF during the wake session measured 42.7 and 49.1 ml/100 g/min, and during the sleep session measured 46.3 and 50.7 ml/100 g/min, representing increases of 8.5 % and 3.2 % relative to wake, respectively. The ROIs that showed significant CBF reductions in the sleeping participants were applied to the non-sleepers' CBF maps. In these ROIs, the sleeping participants exhibited a mean change of −24.2 % during the sleep session, whereas the non-sleepers' ROI CBF values were 41.3 and 49.6 ml/100 g/min during wake and 44.7 and 49.3 ml/100 g/min during the sleep session, corresponding to changes of +8.3 % and −0.6 %, respectively. HF-HRV during the ASL acquisition decreased by 9.7 % and 2.4 % in the two non-sleepers, while the sleeping participants showed a mean HF-HRV increase of 13.5 % during the sleep session.

4. Discussion

4.1. Summary of key findings

This study investigated CBF changes between wakefulness and sleep using ASL. We observed a significant global reduction in GM and WM CBF during sleep, with GM CBF decreasing by 17.0 % and WM by 12.7 %. Voxel-wise analysis revealed region-specific reductions in CBF, most notably in the anterior and posterior cingulate cortex, orbitofrontal and medial prefrontal cortex, precuneus, insula, thalamus, and caudate nucleus. These regions overlap substantially with areas previously shown to be deactivated during SWS in PET studies (Braun et al., 1997; Maquet et al., 1997; Hofle et al., 1997; Kajimura et al., 1999). Notably, the thalamus showed among the most consistent reductions, in line with previous PET findings and studies linking thalamic hypoperfusion to delta rhythm generation (Hofle et al., 1997; Steriade and Amzica, 1998).

We also observed significant reductions in CBF within small but functionally critical brainstem nuclei of the AAN, including the Locus Coeruleus (29.4 % reduction), Medial Reticular Formation (22.8 %), Pontis Oralis (23.4 %), and the Pedunculopontine Nucleus (20.8 %). These reductions survived Bonferroni correction, providing strong evidence that sleep leads to measurable suppression in subcortical regions essential for arousal and state switching. However, caution is warranted in interpreting these findings, as these nuclei are small (comprising only a few ASL voxels in native space), and our ASL protocol was not optimized specifically for brainstem imaging. Still, the consistency of these effects across individuals strengthens the validity of these observations.

4.2. Regional CBF reductions and functional relevance

The regions showing CBF decreases during sleep encompass key components of both the sleep-regulatory systems and default mode network (DMN). For example, the medial prefrontal cortex, posterior cingulate, and precuneus—regions of high metabolic activity during rest—showed reduced CBF during sleep. These DMN nodes are involved in internally directed cognition and are also among the first to show reduced functional connectivity in NREM sleep, consistent with a breakdown of integrative processing and the emergence of local sleep (Horovitz et al., 2009; Sämann et al., 2011). Other areas, including the orbitofrontal cortex, thalamus, and basal ganglia, have been implicated in slow-wave generation (Steriade and Amzica, 1998; Massimini et al., 2004; Lazarus et al., 2013). Although we did not observe any significant regional increases in CBF during sleep, such as those reported in occipital areas by Braun et al. (1997) and Tüshaus et al. (2017), methodological differences across studies (e.g., sleep staging, deprivation protocols, pharmacological induction of sleep) could account for these discrepancies.

4.3. Ascending arousal network and brainstem perfusion

Our exploratory ROI-based analysis of the AAN highlighted significant CBF decreases in brainstem regions that are central to sleep-wake transitions. The Locus Coeruleus, as the primary source of cortical noradrenaline, is vital for arousal, attention, and modulation of the glymphatic system (Aston-Jones & Waterhouse, 2016; Xie et al., 2013). Similarly, the medial reticular formation and pontis oralis nuclei are known to influence cardiovascular, motor, and cognitive functions, and are connected to thalamic systems modulating consciousness and sleep (Saladin, 2018). While these findings are promising, the inherent limitations of ASL in imaging small brainstem nuclei, along with inter-subject anatomical variability—necessitate cautious interpretation. Future studies with higher-resolution ASL or optimized brainstem imaging sequences will be needed to validate these results further.

4.4. ASL as a tool for sleep research

With the exception of a single study by Tüshaus et al. (2017), which directly measured CBF during sleep using simultaneous EEG and ASL, most prior studies investigating perfusion during sleep have relied on PET. PET is widely considered the gold standard for measuring absolute perfusion but has notable limitations, including radiation exposure, the short half-life of ^{15}O, and the need for a cyclotron, making repeated or prolonged sleep recordings challenging. Tüshaus et al. (2017) uniquely demonstrated the feasibility of combining EEG with ASL, revealing heterogeneous CBF dynamics during transitions between N1, N2, and N3 sleep stages. By contrast, Elvsåshagen et al. (2019) used ASL to examine pre- and post-sleep CBF changes, but participants did not sleep during scanning, highlighting our study as only the second study to assess sleep CBF directly using ASL. Our findings reinforce ASL's utility for studying sleep-related neurophysiology, as it allows detection of both global and regional CBF changes across cortical and subcortical areas. The strong agreement with earlier PET studies (Braun et al., 1997; Maquet et al., 1997) further supports ASL's validity and highlights its potential as a powerful neuroimaging tool for future sleep research.

4.5. Comparison with previous studies

Our observed 17.0 % decrease in grey matter CBF during sleep lies between the 26 % reduction reported by Braun et al. (1997) when comparing pre-sleep wakefulness (following sleep deprivation) and SWS, and the 11.4 % reduction found between SWS and post-sleep wakefulness. This discrepancy can be explained by several factors, including differences in sleep pressure, sleep stage, and CBF measurement techniques. For instance, in our study, participants were scanned after a night of regular sleep (wake scan) and after 24 h of sleep deprivation followed by Zolpidem-induced sleep (sleep scan). By contrast, Braun et al. used prolonged sleep deprivation (24–54 h) and PET imaging, which may have led to more pronounced changes. Our use of ASL likely contributes to higher grey matter perfusion estimates (59.7 ml/100 g/min during wakefulness), compared to ~54 ml/100 g/min in Braun's pre-sleep wake condition, and supports the interpretation that participants in our study reached deep sleep stages.

Tüshaus et al. reported lower grey matter CBF values (~43 ml/100 g/min pre-sleep and ~38 post-sleep). They reported a decrease in CBF with sleep initiation and progression (stage 1 and 2), with deep sleep associated with an increase in CBF with respect to light sleep. This contrasts with PET studies that have consistently reported global CBF reductions in SWS. Differences in experimental protocols, such as sleep staging, deprivation duration, and timing of post-sleep wake measurements, may account for these inconsistencies. Moreover, the finding of increased CBF during deeper stages may reflect methodological issues or the influence of transition states rather than stable SWS.

4.6. Sleep manipulation and sleep state inference

Actigraphy confirmed that sleep deprivation was largely successful, although three participants dozed briefly. These individuals did not differ significantly on behavioural or physiological metrics and were retained. Sleepiness ratings prior to the sleep scan and behavioural performance on a button-press task confirmed decreased vigilance during sleep. This was further substantiated by HRV data showing a significant increase in high-frequency power, indicating greater parasympathetic tone, a hallmark of NREM sleep (Vanoli et al., 1995). However, we could not directly determine sleep stage due to the lack of EEG measure.

4.7. Limitations and pharmacological considerations

As single-PLD ASL was used, the observed signal reductions cannot be disentangled from potential effects of arterial transit time; although the chosen PLD (1800 ms) is appropriate for a young, healthy sample, residual sensitivity to transit-time variation remains, this should be considered a confound that can only be resolved with multi-PLD acquisitions. Similar considerations apply to the potential effect of labeling efficiency. As the physiology that influences labeling efficiency (e.g., arterial blood velocity) may vary between sessions, it is possible that small differences in labeling efficiency cannot be excluded. Nevertheless, if our results were explained solely by this, we would expect the differences to act as a global scaling factor rather than produce the regionally specific and sleep-dependent CBF reductions observed here. Another limitation to our study is the use of both sleep deprivation and Zolpidem to facilitate sleep. Although this approach increases the probability of entering sleep during scanning, it may not reflect naturalistic sleep architecture. The observed decreases in CBF are unlikely to reflect sleep deprivation effects alone, as acute deprivation has been associated with heterogeneous CBF responses in humans, ranging from regional hypoperfusion to preserved or increased perfusion depending on arousal state and deprivation duration (Zhou et al., 2019; Elvsåshagen et al., 2019). While some studies report reduced perfusion following prolonged total sleep deprivation (Zhou et al., 2019), others show stable or increased CBF when individuals remain awake (Elvsåshagen et al., 2019). Thus, sleep deprivation may introduce some variability in perfusion but is unlikely to account for the large, widespread CBF reductions observed here. This interpretation is supported by our non-sleeping participants, who underwent the same deprivation protocol yet showed small increases or negligible CBF changes and no rise in HF-HRV, whereas sleeping participants exhibited substantial CBF reductions together with marked parasympathetic dominance. Together, these findings suggest that the perfusion changes primarily reflect sleep-related physiology rather than deprivation alone. Zolpidem effects have also been shown to reduce CBF in certain subcortical regions such as the basal ganglia and insula while increasing it in parietal areas (Finelli et al., 2000), suggesting region-specific pharmacological modulation. In addition, Zolpidem modifies sleep architecture, shifting it toward increased N2, relatively stable or slightly altered N3, and reduced REM, and alters spectral power (Brunner et al., 1991; Besset et al., 1995). Zolpidem has also been shown to alter NREM EEG power distribution, producing an anterior reduction in slow-wave and theta-band power and a posterior shift in 7.8–9.8 Hz activity after sleep deprivation (Landolt et al. 2000). To further explore whether the observed effects could be attributed to the sleep-inducing protocol rather than sleep itself, two participants who did not achieve sleep despite undergoing sleep deprivation and Zolpidem administration were analysed separately. In these non-sleepers, both global and ROI CBF demonstrated small increases or negligible changes relative to wakefulness, and HF-HRV did not exhibit an increase. In contrast, the sleeping group displayed large, widespread CBF reductions accompanied by HF-HRV increases. While the small number of non-sleepers precludes definitive conclusions, these findings suggest that the

principal perfusion and autonomic changes are more likely to reflect sleep-dependent physiology rather than being solely protocol-related. Nonetheless, our overall pattern of results aligns well with prior PET studies of natural SWS, supporting the validity of our findings. Finally, the study sample consisted of young, healthy adults, which limits the generalizability of our findings.

5. Conclusion

Our study provides robust evidence that pharmacologically induced sleep leads to widespread reductions in cerebral perfusion, including in arousal-related brainstem nuclei. These findings converge with prior PET results and extend the literature by showing that ASL is a sensitive tool for detecting sleep-related CBF changes. Importantly, ASL offers a non-invasive, radiation-free, and repeatable method suitable for exploring sleep neurophysiology under physiological and clinical conditions. Future studies incorporating direct EEG measures and improved spatial resolution will be critical in mapping the fine dynamics of sleep-dependent neurovascular changes.

Data and code availability

Data and code are available upon request and after the approval of Brighton and Sussex Medical School Research Governance and Ethics Committee.

Funding sources

This study was funded by Sussex Neuroscience and by University of Sussex Research and Development Fund.

CRediT authorship contribution statement

Balázs Örzsik: Writing – original draft, Visualization, Methodology, Investigation, Formal analysis, Conceptualization. **Iris Asllani:** Writing – review & editing, Supervision, Methodology. **Derk-Jan Dijk:** Methodology. **Neil A Harrison:** Writing – review & editing, Supervision, Methodology, Conceptualization. **Mara Cercignani:** Writing – review & editing, Supervision, Resources, Methodology, Conceptualization.

Declaration of competing interest

None.

Acknowledgments

DJD is supported by the UK Dementia Research Institute [award numbers UKDRI-7005, DRI-CORE2020-CRT, CF2023/7] through UK DRI Ltd, principally funded by the UK Medical Research Council, and additional funding partner Alzheimer's Society.

References

Akerstedt, T., Gillberg, M., 1990. Subjective and objective sleepiness in the active individual. Int. J. Neurosci. 52 (1–2), 29–37.
Alhola, P., Polo-Kantola, P., 2007. Sleep deprivation: impact on cognitive performance. Neuropsychiatr Dis Treatm 3 (5), 553–567.
Alsop, D., Detre, J., Golay, X., Günther, M., Hendrikse, J., Hernandez-Garcia, L., Lu, H., MacIntosh, B., Parkes, L., Smits, M., van Osch, M., Wang, D., Wong, E., Zaharchuk, G., 2015. Recommended implementation of arterial spin-labeled perfusion MRI for clinical applications: a consensus of the ISMRM perfusion study group and the European consortium for ASL in dementia. Magn. Reson. Med. 73 (1), 102–116.
Andersson, J., Onoe, H., Hetta, J., Lidström, K., Valind, S., Lilja, A., Sundin, A., Fasth, K., Westerberg, G., Broman, J., Watanabe, Y., Långström, B., 1998. Brain networks affected by synchronized sleep visualized by positron emission tomography. J. Cereb. Blood Flow Metab. 18 (7), 701–715.
Besset, A., Tafti, M., Villemin, E., Borderies, P., Billiard, M., 1995. Effects of zolpidem on the architecture and cyclical structure of sleep in poor sleepers. Drugs Exp. Clin. Res. 21 (4), 161–169.
Braun, A., Balkin, T.J., Wesenten, N.J., Carson, R.E., Varga, M., Baldwin, P., Selbie, S., Belenky, G., Herscovitch, P., 1997. Regional cerebral blood flow throughout the sleep-wake cycle. An H2(15)O PET study. Brain 120 (7), 1173–1197.
Buchsbaum, M., Hazlett, E.A., Bunney, W.E., 2001. Positron emission tomography with deoxyglucose-F18 imaging of sleep. Neuropsychopharmacology 25 (5 Suppl), S50–S56.
Brunner, D.P., Dijk, D.J., Münch, M., Borbély, A.A., 1991. Effect of zolpidem on sleep and sleep EEG spectra in healthy young men. Psychopharmacol 104 (1), 1–5.
Buysse, D.J., Reynolds 3rd, C.F., Monk, T.H., Berman, S.R., Kupfer, D.J., 1989. The Pittsburgh Sleep Quality Index: a new instrument for psychiatric practice and research. Psychiatry Res. 28 (2), 193–213.
Buzsáki, G., 1998. Memory consolidation during sleep: a neurophysiological perspective. J. Sleep. Res. 7 (S1), 17–23.
Dang-Vu, T., Desseilles, M., Laureys, S., Degueldre, C., Perrin, F., Phillips, C., Maquet, P., Peigneux, P., 2005. Cerebral correlates of delta waves during non-REM sleep revisited. Neuroimage 28 (1), 14–21.
Edlow, B., Takahashi, E., Wu, O., Benner, T., Dai, G., Bu, L., Grant, P., Greer, D., Greenberg, S., Kinney, H., Folkerth, R., 2012. Neuroanatomic connectivity of the human ascending arousal system critical to consciousness and its disorders. J. Neuropathol. Exp. Neurol. 71 (6), 531–546.
Elvsåshagen, T., Mutsaerts, H., Zak, N., Norbom, L., Quraishi, S., Pedersen, P., Malt, U., Westlye, L., van Someren, E., Bjørnerud, A., Groote, I., 2019. Cerebral blood flow changes after a day of wake, sleep, and sleep deprivation. Neuroimage 186, 497–509.
Finelli, L., Landolt, H., Buck, A., Roth, C., Berthold, T., Borbély, A., Achermann, P., 2000. Functional neuroanatomy of human sleep states after zolpidem and placebo: a H215O-PET study. J. Sleep. Res. 9 (2), 161–173.
Fultz, N., Bonmassar, G., Setsompop, K., Stickgold, R., Rosen, B., Polimeni, J., Lewis, L., 2019. Coupled electrophysiological, hemodynamic, and cerebrospinal fluid oscillations in human sleep. Science 366 (6465), 628–631.
Hofle, N., Paus, T., Reutens, D., Fiset, P., Gotman, J., Evans, A., Jones, B., 1997. Regional cerebral blood flow changes as a function of delta and spindle activity during slow wave sleep in humans. J. Neurosci. 17 (12), 4800–4808.
Horovitz, S.G., Braun, A.R., Carr, W.S., Picchioni, D., Balkin, T.J., Fukunaga, M., Duyn, J. H., 2009. Decoupling of the brain's default mode network during deep sleep. Proc. Natl. Acad. Sci. 106 (27), 11376–11381.
Iliff, J., Nedergaard, M., 2013. Is there a cerebral lymphatic system? Stroke 44 (6, Supplement 1), S93–S95.
Kajimura, N., Uchiyama, M., Takayama, Y., Uchida, S., Uema, T., Kato, M., Sekimoto, M., Watanabe, T., Nakajima, T., Horikoshi, S., Ogawa, K., Nishikawa, M., Hiroki, M., Kudo, Y., Matsuda, H., Okawa, M., Takahashi, K., 1999. Activity of midbrain reticular formation and neocortex during the progression of Human non-rapid eye movement sleep. J. Neurosci. 19 (22), 10065–10073.
Landolt, H., Finelli, L.A., Roth, C., Buck, A., Achermann, P., Borbély, A.A., 2000. Zolpidem and sleep deprivation: different effect on EEG power spectra. J. Sleep. Res. 9 (2), 175–183.
Lazarus, M., Chen, J., Urade, Y., Huang, Z., 2013. Role of the basal ganglia in the control of sleep and wakefulness. Curr. Opin. Neurobiol. 23 (5), 780–785.
Luyster, F., Strollo, P., Zee, P., Walsh, J., 2012. Sleep: a health imperative. Sleep 35 (6), 727–734.
Maquet, P., Degueldre, C., Delfiore, G., Aerts, J., Péters, J., Luxen, A., Franck, G., 1997. Functional neuroanatomy of Human slow wave sleep. J. Neurosci. 17 (8), 2807–2812.
Massimini, M., Huber, R., Ferrarelli, F., Hill, S., Tononi, G., 2004. The sleep slow oscillation as a traveling wave. J. Neurosci. 24 (31), 6862–6870.
Monti, J.M., Spence, D.W., Buttoo, K., Pandi-Perumal, S.R., 2017. Zolpidem's use for insomnia. Asian J. Psychiatr. 25, 79–90.
Nofzinger, E., Buysse, D., Miewald, J., Meltzer, C., Price, J., Sembrat, R., Ombao, H., Reynolds, C., Monk, T., Hall, M., Kupfer, D., Moore, R., 2002. Human regional cerebral glucose metabolism during non-rapid eye movement sleep in relation to waking. Brain 125 (5), 1105–1115.
Örzsik, B., 2022. Using Multi-Modal MRI Techniques to Measure Glymphatic Function In-Vivo. University of Sussex. PhD thesis.
Örzsik, B., Palombo, M., Asllani, I., Dijk, D.-J., Harrison, N.A., Cercignani, M., 2023. Higher order diffusion imaging as a putative index of human sleep-related microstructural changes and glymphatic clearance. Neuroimage 274, 120124.
Palmer, C.A., Alfano, C.A., 2017. Sleep and emotion regulation: an organizing. Integr. Rev. Sleep Med. Rev. 31, 6–16.
Priest, R., Terzano, M., Parrino, L., Boyer, P., 1997. Efficacy of zolpidem in insomnia. Eur. Psychiatry 12 (S1), 4S–14S.
Rechtschaffen, A., Bergmann, B., 2002. Sleep deprivation in the rat: an update of the 1989 paper. Sleep 25 (1), 18–24.
Rolls, E.T., Huang, C., Lin, C., Feng, J., Joliot, M., 2019. Automated anatomical labelling atlas 3. Neuroimage 206, 116189.
Saladin, K.S., 2018. Chapter 14 - the brain and cranial nerves. Anatomy and Physiology: The Unity of Form and Function, 8th ed. McGraw-Hill, New York. The Reticular Formation, 518-519.
Sämann, P.G., Wehrle, R., Hoehn, D., Spoormaker, V.I., Peters, H., Tully, C., Holsboer, F., Czisch, M., 2011. Development of the brain's default mode network from wakefulness to slow wave sleep. Cereb. Cortex. 21 (9), 2082–2093.
Stephenson, R., Chu, K., Lee, J., 2007. Prolonged deprivation of sleep-like rest raises metabolic rate in the Pacific beetle cockroach, Diploptera punctata (Eschscholtz). J. Exp. Biol. 210 (14), 2540–2547.
Steriade, M., Amzica, F., 1998. Coalescence of sleep rhythms and their chronology in corticothalamic networks. Sleep. Res. Online 1 (1), 1–10.

Tononi, G., Cirelli, C., 2014. Sleep and the price of plasticity: from synaptic and cellular homeostasis to memory consolidation and integration. Neuron 81 (1), 12–34.
Tüshaus, L., Omlin, X., Tuura, R., Federspiel, A., Luechinger, R., Staempfli, P., Koenig, T., Achermann, P., 2017. In human non-REM sleep, more slow-wave activity leads to less blood flow in the prefrontal cortex. Sci. Rep. 7 (1).
Vanoli, E., Adamson, P., Ba-Lin, Pinna, G., Lazzara, R., Orr, W., 1995. Heart rate variability during specific sleep stages. Circulation 91 (7), 1918–1922.
Wickens, C., Hutchins, S., Laux, L., Sebok, A., 2015. The impact of sleep disruption on complex cognitive tasks. Hum. Factors: J. Hum. Factors Ergon. Soc. 57 (6), 930–946.
Xie, L., Kang, H., Xu, Q., Chen, M., Liao, Y., Thiyagarajan, M., O'Donnell, J., Christensen, D., Nicholson, C., Iliff, J., Takano, T., Deane, R., Nedergaard, M., 2013. Sleep drives metabolite clearance from the adult brain. Science 342 (6156), 373–377.
Zhou, F., Huang, M., Gu, L., Hong, S., Jiang, J., Zeng, X., Gong, H., 2019. Regional cerebral hypoperfusion after acute sleep deprivation: a pseudo-continuous arterial spin labeling study. Med 98 (6), e14309.
Zimmerman, J., Naidoo, N., Raizen, D., Pack, A., 2008. Conservation of sleep: insights from non- mammalian model systems. Trends. Neurosci. 31 (7), 371–376.